Electronic Supplementary Material (ESI) for Nanoscale.
This journal is © The Royal Society of Chemistry 2015

Role of the heterojunctions in In_2O_3-composited SnO_2 nanorod sensors and their remarkable gas-sensing performance for NO_x at room temperature

Shuang Xu[a], Jun Gao[a], Linlin Wang[a], Kan Kan[a], Yu Xie[c], Peikang Shen[d], Li Li[a, b] and Keying Shi*[a, e]*

a Key Laboratory of Functional Inorganic Material Chemistry, Ministry of Education. Key Laboratory of Physical Chemistry, School of Chemistry and Material Science, Heilongjiang University, Harbin, 150080, P. R. China.

b Key Laboratory of Chemical Engineering Process＆Technology for High-efficiency Conversion，School of Chemistry and Material Science, Heilongjiang University, Harbin 150080, P. R. China

c Department of Materials Chemistry, Nanchang Hangkong University, Nanchang, 330063, P. R. China.

d Department of Physics and Engineering Sun Yat-sen University Guangzhou, 510275, P. R. China.

e Department of Mechanical Engineering, University of Wisconsin-Milwaukee, 3200 North Cramer Street, Milwaukee, Wisconsin 53211, United States.

E-mail:shikeying2008@163.com; llwjjhlju@sina.cn; Fax: (+86) 451 8667 3647; Tel: (+86) 451 8660 9141

The I_{ds}-V_{ds} measurements device equipped with two removable probes placed directly on the electrode contact areas on the substrate, as shown in Figure S1. The interdigital Au electrode spacing is 2 μm

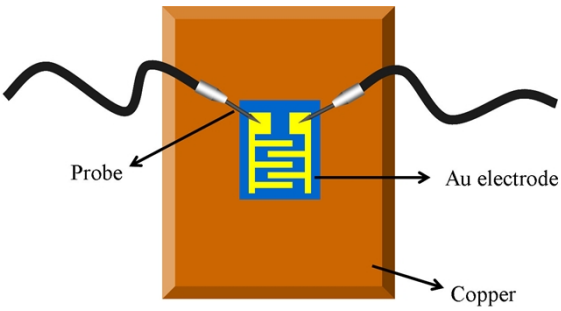

Figure S1 Device structure of I_{ds}-V_{ds} measurement

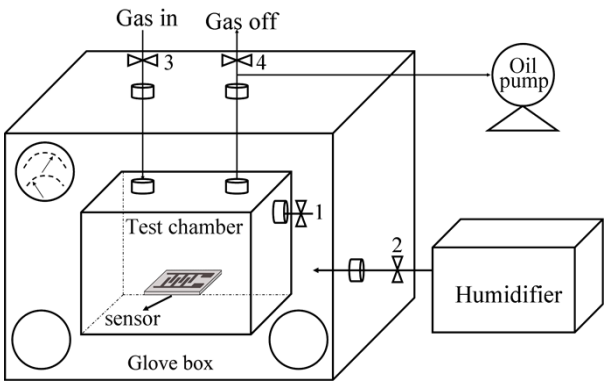

Figure S2 The diagram of the gas delivery system for the gas sensing process

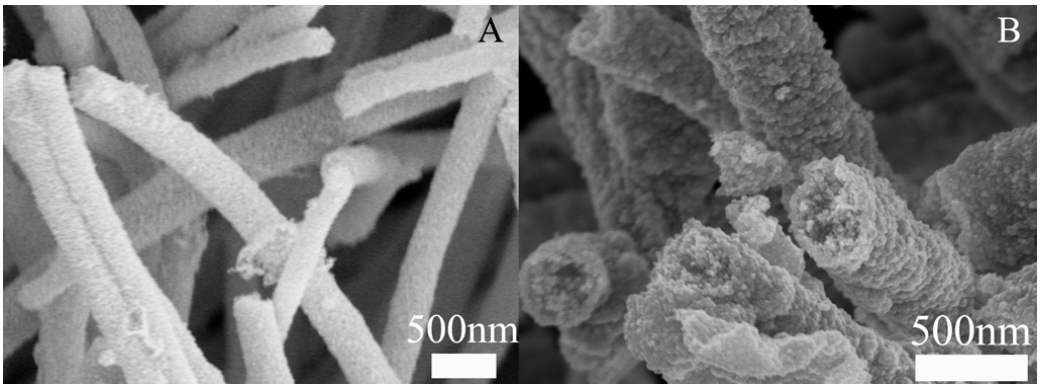

Figure S3 SEM image of (A) 1ICTO and (B) 5ICTO.

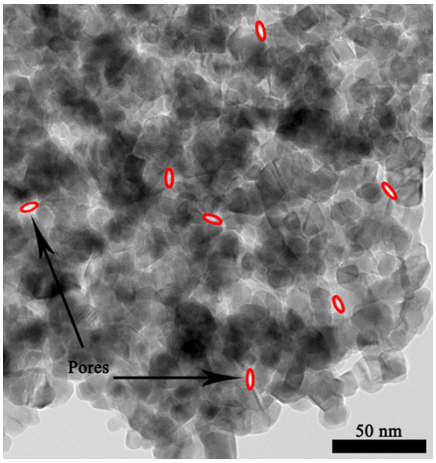

Figure S4 TEM image of 3ICTO. The arrows point out pores. The SnO_2 nanoparticles (NPs) dispersed on the surface of 3ICTO. The sizes of SnO_2 NPs is about 5-20 nm (see the diameter distribution of 3ICTO in Figure S6B).

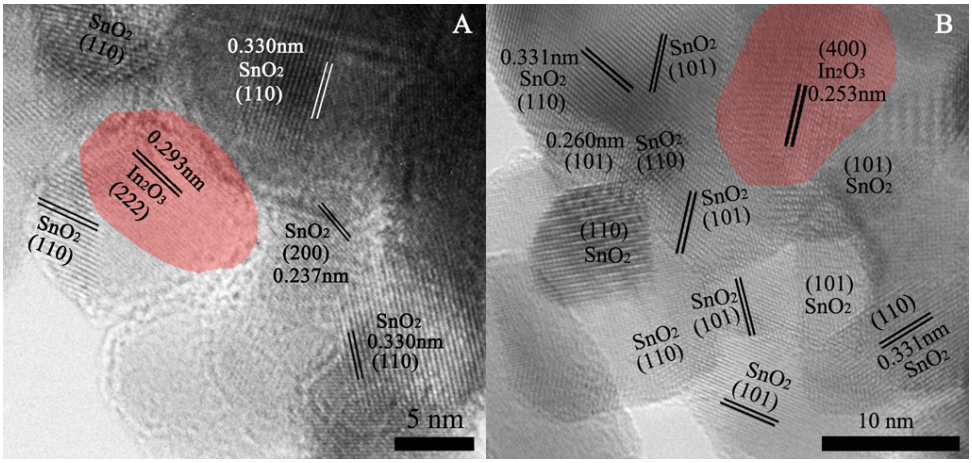

Figure S5 HRTEM images of (A) 1ICTO and (B) 5ICTO in which (110), (200) and (101) planes of SnO_2, (222) and (400) planes of In_2O_3 can be seen.

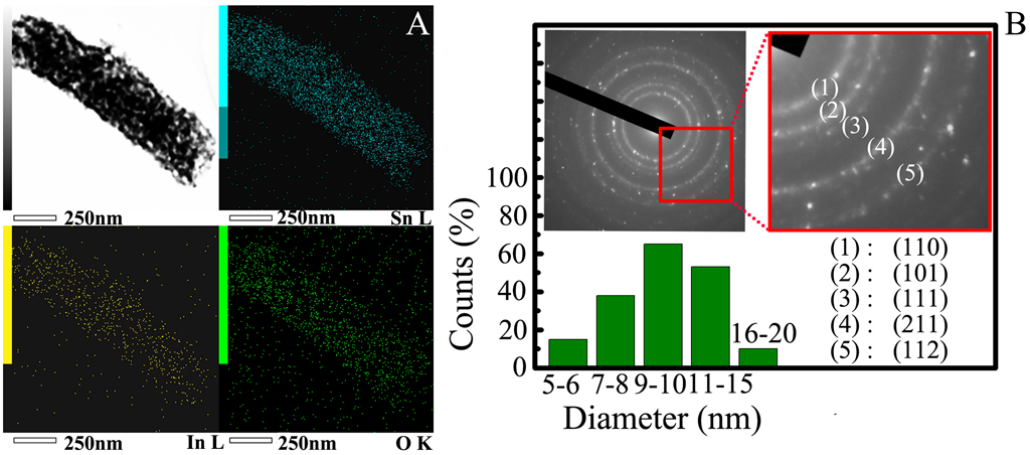

Figure S6 (A) element maps of the 3ICTO NRs (B) the nanoparticles diameter distribution of 3ICTO NRs, the inset of (B) shows the SAED pattern of SnO_2 NPs

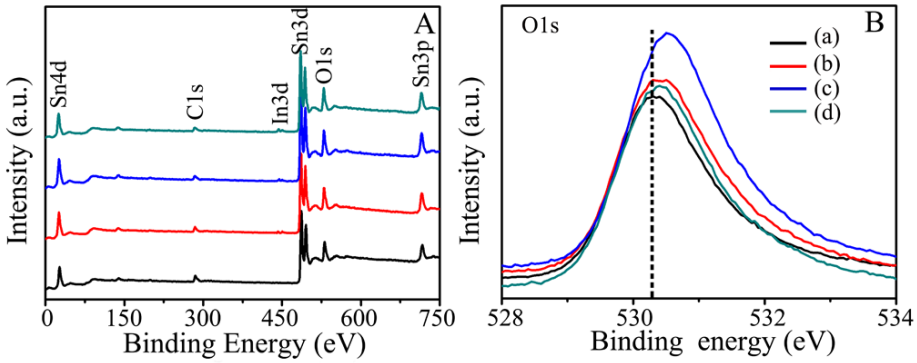

Figure S7 The XPS full spectra (A) and O1s spectra of (B): (a) pristine SnO_2, (b) 1ICTO, (c) 3ICTO, (d) 5ICTO

Table S1. XPS results of pristine In_2O_3 and various ICTOs

	Banding energy (eV)	
samples	$In3d_{5/2}$	$In3d_{3/2}$
In_2O_3	443.8	451.4
1ICTO	444.6	452.2
3ICTO	444.8	452.4
5ICTO	444.8	452.4

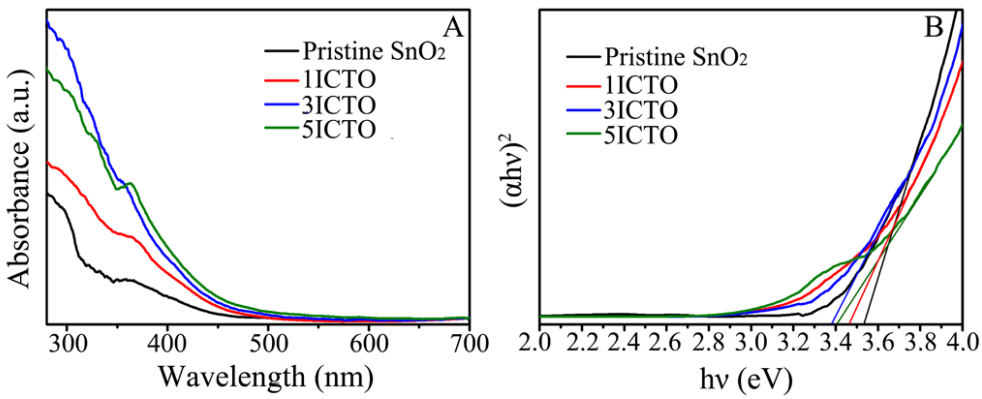

Figure S8 (A) UV–vis diffuse reflection–absorption curves; (B) plot of $(\alpha h\nu)^2$ versus incident photon energy ($h\nu$) for the ICTOs (the pristine SnO_2 (black line) and1ICTO (red line), 3ICTO (blue line), and 5ICTO (green line))

The band gap energy of a semiconductor could be calculated by equation (eq) 1[1]

$$\alpha h\nu = K(h\nu - E_g)^n \qquad (1)$$

Where E_g is the band gap energy, hν is the incident photon energy, K is a constant, α is the absorption coefficient. In the eq.1, n decides the characteristics of the transition in a semiconductor. In the case of SnO_2, the value of n is 1 due to a direct optical transition type for SnO_2. Therefore, by plotting $(\alpha h\nu)^2$ versus hν, the band gap (E_g) can be determined (as shown in Figure S8B).

The carrier concentration also can be calculated by the slope of the MS curves using the following eq2.

$$N_d = (2/e_0\varepsilon\varepsilon_0)\left[d(1/C^2)/dV\right]^{-1} \qquad (2)$$

where e_0 is the fundamental charge constant, ε_0 is the permittivity of vacuum, ε is the relative permittivity of SnO_2 (ε=23.4)[2]

Table S2 Carrier concentrations and fitted impedance parameters of the SnO_2, 1ICTO, 3ICTO and 5ICTO

Samples	$R_Q(\Omega)$	$R_{ct}(\Omega)$	$N_d(cm^{-3})$
SnO_2	540.8	6130	3.25×10^{19}
1ICTO	403.3	3186	3.79×10^{19}
3ICTO	263.8	116.6	9.32×10^{19}
5ICTO	334.5	138.6	4.46×10^{19}

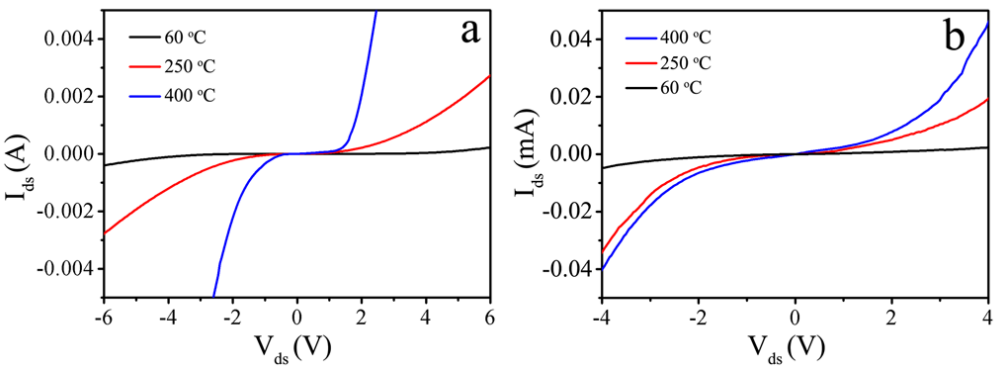

Figure S9 I-V curves measured at RT for (a) 3ICTO and (b) pristine SnO_2 thin film sensors, which were treated at 60 °C, 250 °C and 400 °C in Ar

Figure S9 shows the current-voltage (I_{ds}-V_{ds}) characteristics for a 3ICTO and pristine SnO_2 were measured by sweeping the drain voltage from -10 V to 10 V with constant V_g=1.0 V in 0.05 V steps.

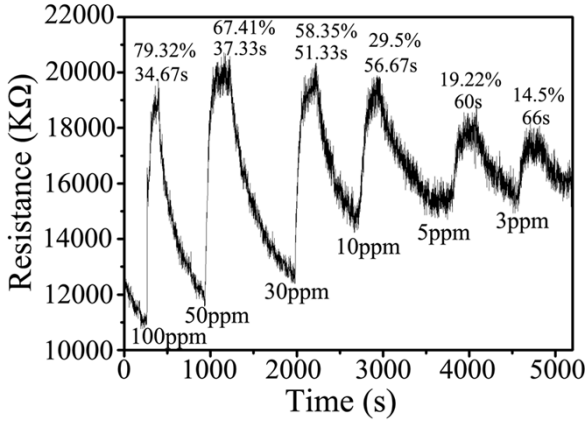

Figure S10 Dynamic response-recovery curves of the pristine SnO_2 sensor to 100 ppm-3 ppm NO_x at RT

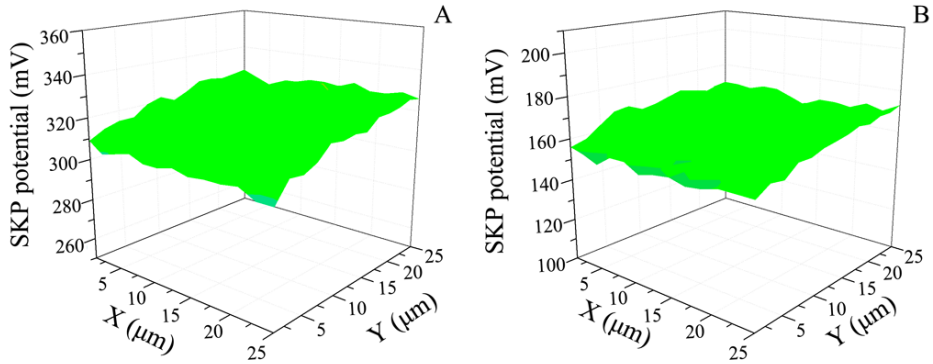

Figure S11 Work functions of the (A) pristine SnO_2 and (B) pristine In_2O_3

References

[1] J. Lv, T. Kako, Z. S. Li, Z. G. Zou and J. H. Ye, *J. Phys. Chem. C*, 2010, **114**, 6157-6162

[2] A. Ishikawa, T. Takata, J. N. Kondo, M. Hara, H. Kobayashi and K. Domen, *J. AM. CHEM. SOC.*, 2002, **124**, 13547–13553